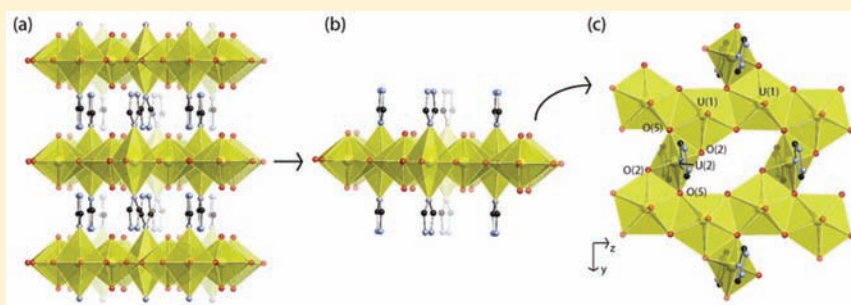


$(\text{UO}_2)_2[\text{UO}_4(\text{trz})_2](\text{OH})_2$: A U(VI) Coordination Intermediate between a Tetraoxido Core and a Uranyl Ion with Cation–Cation Interactions

Zhehui Weng,[†] Shuao Wang,[†] Jie Ling,[†] Jessica M. Morrison,[†] and Peter C. Burns^{*,†,‡}

[†]Department of Civil Engineering and Geological Sciences and [‡]Department of Chemistry and Biochemistry, University of Notre Dame, Notre Dame, Indiana 46556, United States

S Supporting Information



ABSTRACT: A uranyl triazole $(\text{UO}_2)_2[\text{UO}_4(\text{trz})_2](\text{OH})_2$ (**1**) ($\text{trz} = 1,2,4\text{-triazole}$) was prepared using a mild solvothermal reaction of uranyl acetate with 1,2,4-triazole. Single-crystal X-ray diffraction analysis of **1** revealed it contains sheets of uranium–oxygen polyhedra and that one of the U(VI) cations is in an unusual coordination polyhedron that is intermediate between a tetraoxido core and a uranyl ion. This U(VI) cation also forms cation–cation interactions (CCIs). Infrared, Raman, and XPS spectra are provided, together with a thermogravimetric analysis that demonstrates breakdown of the compound above 300 °C. The UV–vis–NIR spectrum of **1** is compared to those of another compound that has a range of U(VI) coordination environments.

1. INTRODUCTION

The linear $(\text{UO}_2)^{2+}$ uranyl ion is dominant in the coordination chemistry of U(VI).^{1,2} It is typically coordinated by 4–6 ligands arranged in equatorial positions of square, pentagonal, and hexagonal bipyramids that are capped by the O atoms of the uranyl ion.³ These bipyramids often link into sheet structural units by sharing equatorial edges with each other or sharing equatorial edges or vertices with other oxyanions.⁴ The uranyl ion O atoms seldom form bonds within the structural unit.^{3,5} However, recent studies demonstrated unexpected reactivity of this normally unreactive functional group.^{6–10}

Several studies have examined the rare occurrence of cation–cation interactions (CCIs) in U(VI) uranyl compounds.^{11–19} In actinide chemistry, a CCI occurs where an O atom of a donor actinyl ion coordinates an acceptor actinyl ion in the equatorial plane of its corresponding bipyramid. CCIs were first observed and designated as such in solution between neptunyl and uranyl ions in 1961,²⁰ and the designation has been in steady usage since then, although the interaction between the two actinyl ions is through an O atom. CCIs are common where the actinyl ions contain pentavalent cations, such as Np(V), U(V), Pu(V), and Am(V).^{4,21–24} They create novel linkages among building units that often result in framework structures.^{2,4,24–28} CCIs are also important in impacting the chemical and physical properties, such as the disproportionation of $An(V)$, and magnetic ordering and electronic absorption in some Np(V)

compounds.^{25,29,30} CCIs rarely occur where the actinyl ion contains a hexavalent cation, although a few U(VI) compounds with CCIs have been synthesized, most of which adopt framework structures.^{11–13,16} CCIs can be defined as two or three centered in which the CCI is accepted by one ($\mu_2\text{-oxo}$) or two ($\mu_3\text{-oxo}$) acceptors. Most CCIs are two centered. Five examples of three-center CCIs containing U(VI) or Np(V) are known: $\text{Sr}_5(\text{UO}_2)_{20}(\text{UO}_6)_2\text{O}_{16}(\text{OH})_6(\text{H}_2\text{O})_6$,¹⁹ $(\text{K},\text{Na})\text{-Na}_3[(\text{UO}_2)_5\text{O}_6(\text{SO}_4)]$,³¹ $\text{Li}_4[(\text{UO}_2)_{10}\text{O}_{10}(\text{Mo}_2\text{O}_8)]$,¹⁷ $\text{K}(\text{NpO}_2)_3(\text{H}_2\text{O})\text{Cl}_4$,³⁰ and Np_2O_5 .³²

Tetraoxido core structures for actinides have four short $An\text{-O}$ bond lengths and are known for Np(VII) and Pu(VII).^{3,33,34} There are six examples of tetraoxido $(\text{UO}_4)^{2-}$ ions. In these compounds, the four U-O bond distances range from 1.84 to 2.07 Å,^{35–38} which is much shorter than the $\text{U-O}_{\text{equatorial}}$ distances typical about uranyl ions (around 2.3 Å) and significantly longer than the normal uranyl U=O distance (around 1.79 Å). The reported U(VI) tetraoxido species are located between chains of edge-sharing uranyl pentagonal bipyramids in a specific sheet topology, suggesting that this unusual coordination environment is stabilized by such layer structures.^{35,36}

Received: February 1, 2012

Published: June 11, 2012

We are interested in the role of CCIs and tetraoxido cores in structural topologies and properties of actinyl materials. Here we report the solvothermal synthesis and crystal structure of a novel U(VI)–triazolate complex $(\text{UO}_2)_2[\text{UO}_4(\text{trz})_2](\text{OH})_2$ (**1**) ($\text{trz} = 1,2,4\text{-triazolate}$) that contains a U(VI) coordination environment that is intermediate between a tetraoxido core and a uranyl ion and contains CCIs. Thermogravimetric analysis of **1** shows both a thermally driven U reduction and a subsequent oxidation upon further heating. Absorption spectra of **1** are compared to other U(VI) compounds that contain either CCIs or a tetraoxido core. IR, Raman, and X-ray photoelectron spectra and powder X-ray diffraction pattern of compound **1** are reported.

2. EXPERIMENTAL SECTION

Synthesis. Compound **1** was synthesized solvothermally with uranyl acetate and 1,2,4-triazole. *Caution! Although depleted uranium was used in these studies, standard precautions for handling radioactive materials should be followed.* A mixed solution of ethanol (7 mL), acetonitrile (7 mL), and water (1 mL) containing uranyl acetate (0.5 mmol, 0.2122 g) and 1,2,4-triazole (0.5 mmol, 0.0353 g) was heated at 150 °C in a 23 mL Teflon-lined stainless steel reaction vessel for 4 days, followed by cooling to room temperature at a rate of 10 °C h⁻¹. Yellow block-like crystals of **1** were collected (in ca. 42% yield) by filtration of the reaction mixture and washed with the distilled water.

Single-Crystal X-ray Diffraction. A suitable single crystal of **1** was selected using cross-polarized light. It was mounted on a glass fiber for single-crystal X-ray diffraction studies using a Bruker three-circle single-crystal X-ray diffractometer equipped with an APEX II CCD detector and Mo K α radiation from a conventional sealed tube. A sphere of three-dimensional diffraction data was collected at room temperature using frame widths of 0.5° in ω . Data were integrated and corrected for background, Lorentz, and polarization effects using the APEX II software and corrected for absorption empirically using SADABS. The structure was solved and refined using SHELXTL on the basis of F^2 . Crystal data and details of data collection and structure refinement are given in Table 1, and selected bond lengths are listed in Table 2.

Table 1. Crystallographic Data and Structure Refinement Results for Compound 1

structure formula	$(\text{UO}_2)_2[\text{UO}_4(\text{trz})_2](\text{OH})_2$
fw	1010.20
cryst syst	orthorhombic
space group	<i>Cmca</i>
<i>a</i> (Å)	13.872(3)
<i>b</i> (Å)	13.658(3)
<i>c</i> (Å)	7.5695(15)
<i>V</i> (Å ³)	1434.2(5)
<i>Z</i>	4
ρ_{calcd} (g/cm ³)	4.660
μ (mm ⁻¹)	33.856
R_{int}	0.0486
R_1 [$I > 2\sigma(I)$]	0.0178
wR_2 (all data)	0.0453
GOF on F^2	1.052
$\Delta\rho_{\text{max}}$ $\Delta\rho_{\text{min}}$ (e Å ⁻³)	3.210, -1.491

Infrared and Raman Spectra. An Infrared spectrum was collected from a powdered specimen of **1** using a FT/IR-6300 type A microspectrometer equipped with a ATR PRO450-S objective. The spectrum was taken from 550 to 4000 cm⁻¹ with a beam aperture of 100 μm for crystals that were stored in a desiccator for 24 h prior to analysis. A Raman spectrum was collected at room temperature from a single crystal of **1** using an Alpha300R spectrometer with a 532 nm

excitation laser. WITec software was used for Raman data analysis. Both infrared and Raman spectra are provided in the Supporting Information (Figure S1).

UV–vis–NIR and Fluorescence Spectra. Electronic absorption and fluorescence data were acquired from single crystals of **1** using a Craic Technologies microspectrophotometer with a fluorescence attachment. The UV–vis–NIR spectrum was taken from 250 to 1500 nm. Excitation of compound **1** was achieved using 365 nm light from a mercury lamp.

Thermogravimetric Analysis. Thermogravimetric measurements were done for compound **1** using a Netzsch TG209 F1 Iris thermal analyzer. Samples were loaded into an Al₂O₃ crucible for heating at a rate of 5 °C/min. One sample was heated from 25 to 900 °C, and subsequently, a second sample was heated from 25 to 515 °C.

Powder X-ray Diffraction. Powder X-ray diffraction patterns of compound **1** and the products of heat treatment were collected on a Bruker θ – θ diffractometer equipped with a Lynxeye one-dimensional solid state detector and Cu K α radiation at room temperature over the angular range from 5° to 80° (2θ) with a scanning step width of 0.05° and a fixed counting time of 1 s/step. Collected patterns were compared with those calculated from their structures using Mercury³⁹ (see Figures S3 and S4, Supporting Information).

X-ray Photoelectron Spectrum. X-ray photoelectron spectrum measurements were performed with an XSAM 800 spectrometer with nonmonochromatic Al K α radiation at 1486.6 eV (144 W, 20 eV pass energy). The pressure in the spectrometer was typically 10⁻⁸ Torr. The C 1s peak of adventitious carbon at 284.6 eV was used for callibration.

3. RESULTS

Synthesis. We selected 1,2,4-triazole (trz) as a ligand to coordinate uranyl because it can bridge and chelate metal cations or be a monodentate ligand, as shown in transition-metal-based systems.^{40–43} We are unaware of any other compounds containing actinyl ions coordinated by 1,2,4-triazole. The size and electron-delocalized ring structure of trz may offer alternative tether lengths, different charge-balance requirements, as well as orientations of donor groups.⁴⁴ We are interested in the reaction between 1,2,4-triazole and uranium salts because of the potential for unique bonding motifs.

Compound **1** resulted from reaction of uranyl acetate and 1,2,4-triazole in a mixed solvent of CH₃CH₂OH, CH₃CN, and H₂O under solvothermal conditions. Reaction at 150 °C over 4 days produced yellow block-shaped crystals in 42% yield. Phase purity was confirmed by comparing its simulated and experimental powder X-ray diffraction patterns (Figure S3, Supporting Information).

Crystal Structure. Compound **1** contains two symmetrically distinct U(VI) cations that occur in very different coordination environments. As shown by crystal structure analysis, the U(1) cation occurs as a typical uranyl ion with U=O bond lengths of 1.773(5) Å. The uranyl ion is coordinated by five O atoms that are arranged at the equatorial vertices of a pentagonal bipyramid (Figure 1) with U–O_{eq} bond lengths ranging from 2.328(6) to 2.496(6) Å. The calculated bond-valence sums at the coordinating O(3), O(2), and O(5) sites^{1,45} are 1.07, 1.90, and 2.02 νu , respectively, giving designations as the hydroxyl O(3)H⁻, O(2)²⁻, and O(5)²⁻ units. The U(2) cation is coordinated by four O atoms with two distinct bond lengths, 1.855(7) Å in a trans arrangement [U(2)–O(2)] and 2.077(7) Å also in a trans arrangement [U(2)–O(5)]. The U(2), O(2), and O(5) atoms are coplanar, the O(2)–U(2)–O(2) and O(5)–U(2)–O(5) bond angles are both 180°, and the O(2)–U(2)–O(5) angles are 82.1 and 97.9°. The U(2) cation is further coordinated by

Table 2. Selected Bond Lengths (Angstroms) for Compound 1^a

U(1)–O(1)	1.773(5)	U(1)–O(5)D	2.441(6)	U(2)–N(1)	2.497(8)
U(1)–O(3)B	2.328(6)	U(2)–O(2)	1.855(7)	O(3)–U(1)E	2.328(6)
U(1)–O(5)C	2.330(7)	U(2)–O(5)	2.078(7)	O(5)–U(1)A	2.330(7)
U(1)–O(3)	2.398(6)	U(2)–O(5)D	2.077(7)	U(1)–U(2)	3.5826(6)
U(1)–O(2)	2.496(6)	U(2)–N(1)D	2.497(8)	U(1)–U(1)B	3.8550(7)

^aSymmetry codes: (A) $x, y - 1/2, -z + 3/2$; (B) $-x + 2, -y + 3/2, z - 1/2$; (C) $x, y + 1/2, -z + 3/2$; (D) $-x + 2, -y + 1, -z + 1$; (E) $-x + 2, -y + 3/2, z + 1/2$.

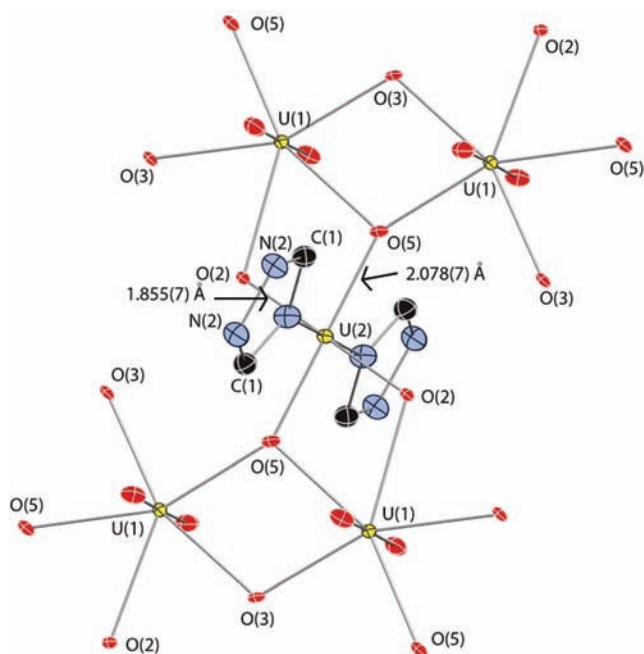


Figure 1. Depiction of the coordination environments of the three U(VI) sites and the CCI in compound 1. Displacement ellipsoids drawn at 50% probability.

two N atoms of trz with a U–N bond length of 2.497(8) Å and a N–U(2)–N bond angle of 180°. The U–N bonds are perpendicular to the plane containing U(2), O(2), and O(5).

The U(2)–O(2) bond lengths are 0.06 Å longer than a typical uranyl ion. U(2) donates single CCIs through both O(2) atoms, each to a single distinct U(1) cation. If the U(2) coordination polyhedron is characterized as a distorted tetraoxido core (see below), the U(2) cation donates double CCIs through each of the O(5) cations, which are accepted by two different U(1) cations. Note that the U(2)=O(5) distance is somewhat longer than the uranyl bond length typically involved in double CCIs.¹⁷ Each U(1) cation accepts a total of three CCIs donated by two U(2) cations. Calculation of bond-valence sums incident at the U(1) and U(2) sites using coordination-specific parameters^{1,45} gives 5.92 and 5.88 νu , respectively, consistent with the formal valence of U(VI).^{11,35}

Table 3 lists uranyl U=O bond distances of several U(VI) compounds with and without CCIs. Whereas the uranyl U=O bond distance of a typical uranyl ion is ~ 1.79 Å, bond distances of uranyl U=O ions that form two- and three-center CCIs are in the range of 1.8–1.9 and 1.93–2.10 Å, respectively. Where there is a U(VI) tetraoxido core,^{35–38} the U–O bond distances corresponding to donation of one and two CCIs are 1.858 and 1.84–2.079 Å, respectively. In previously reported compounds adopting U(VI) tetraoxido core structures, all of the tetraoxido O atoms are involved in three-center CCIs and the bond

Table 3. Selected U–O Bond Distance Ranges in U(VI) Compounds with Different Coordination Modes

Coordination Mode	Bond Distance (Å)	Reference
	~ 1.79	9
	1.8–1.9	11, 12, 16
	1.93–2.10	17, 19, 31
	1.855	compound 1
	1.84–2.079	35–38 compound 1

lengths about the U(VI) cation are similar, with an average bond distance of 1.98 Å. In compound 1, however, both two- and three-center CCIs arguably occur, together with a distorted tetraoxido core structure with an average U–O bond distance of 1.97 Å.

The connectivity of 1 is dominated by the CCIs described above, which link the U(1) and U(2) polyhedra into two-dimensional sheets. The U(1) pentagonal bipyramids share equatorial edges, forming chains that extend along [001] (Figure 2). These chains are linked into sheets through the U(2) cation, the coordination polyhedron of which contributes three of the equatorial vertices of the U(1) bipyramid. The other two equatorial vertices are shared only between the U(1) bipyramids and correspond to hydroxyl ions. The U–U distances in the resulting sheet range from 3.5826(6) to 3.8550(7) Å. The U–U distances are shorter than corresponding distances in most U(VI) compounds.^{17,19}

Each U(2) polyhedron contains an N atom from each of two trz ligands. These are located on either side of the sheet of uranyl polyhedra, where they are directed into the interlayer region (Figure 2). Adjacent sheets are offset to facilitate packing of the trz ligands in the interlayer.

To investigate topological relationships with other structures, the sheet anion topology of 1, created using the method established by Burns et al.,⁴⁶ is shown in Figure S2, Supporting Information. This is the well-known uranophane anion topology that consists of triangles, squares, and pentagons. In most sheets based upon this topology the pentagons contain uranyl ions, giving pentagonal bipyramids, and the triangles correspond to faces of silicate tetrahedra, as in the uranophane group of minerals. In the case of 1, the pentagons also contain uranyl ions but the squares are occupied by U(VI) in a coordination environment that is transitional between a tetraoxido core and a uranyl ion. The structure of hydrogen triuranate also contains sheets of this anion topology with the squares occupied by U in a very similar environment as 1.⁴⁷ Specifically, the U cation in the square of the anion topology is coplanar with four O atoms, with two sets of U–O bond

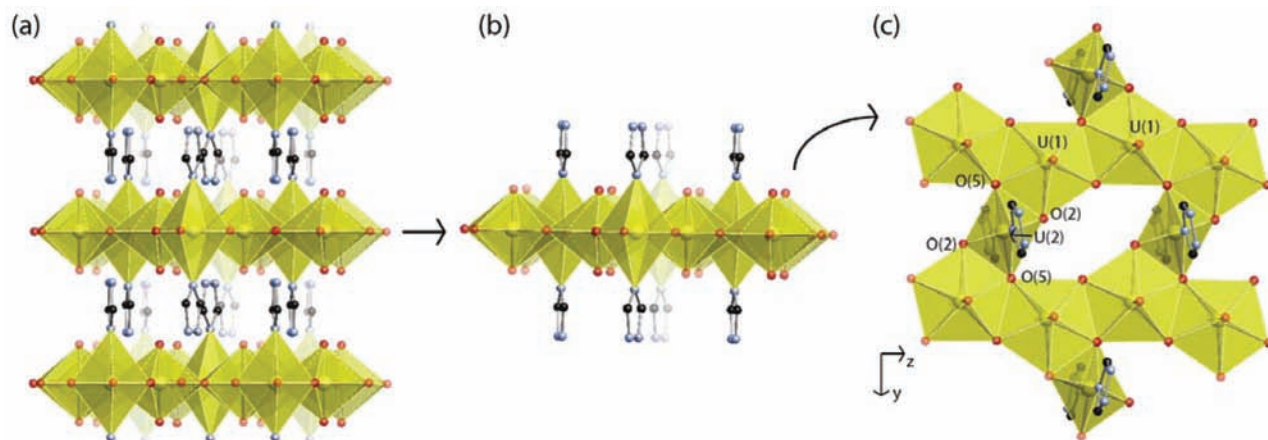


Figure 2. Polyhedral representations of the structure of compound **1**. Uranium polyhedra are shown in yellow. U, C, N, and O atoms are shown as yellow, black, blue, and red spheres, respectively.

lengths at 1.82 and 2.07 Å, indistinguishable within error from those in **1**. In hydrogen triuranate the U cation is also coordinated by two O atoms of adjacent sheets, each at 2.40 Å. In KU_2O_7 , a sheet with the uranophane anion topology occurs in which the pentagons are occupied by uranyl ions and every second square contains a U cation.⁴⁸ The U cation in the squares of the topology has two short U–O bonds extending into the interlayer with distances of 1.85 and 1.93 Å. The equatorial U–O bonds range from 2.15 to 2.21 Å.

IR and Raman Spectra. In the IR spectrum of compound **1** (Figure S1a, Supporting Information) there are no vibration modes detected in the region of 3300–4000 cm^{-1} , and characteristic bands of triazole^{49,50} are present in the range of 640–1600 cm^{-1} . No bands related to the ν_3 (UO_2)²⁺ antisymmetric stretching vibration are present in the Raman spectrum of **1** (Figure S1b, Supporting Information), and infrared bands at 904 and 880 cm^{-1} are assigned to ν_3 (UO_2)²⁺.⁵¹ Raman bands at 837 and 769 cm^{-1} and infrared bands at 839 and 764 cm^{-1} are attributed to the ν_1 (UO_2)²⁺ symmetric stretching vibrations.⁵² Detailed assignments are given in Table S1, Supporting Information.

Bartlett et al.⁵³ provided an empirical relationship for the uranyl ion bond length and the Raman frequency of the corresponding vibrations: $d(\text{U}-\text{O})$ (pm) = 10 650 [ν_1 (cm^{-1})]^{-2/3} + 57.5. The calculated bond lengths in compound **1** are 1.77 and 1.84 Å, consistent with those from crystal structure analysis.

Fluorescence and X-ray Photoelectron Spectrum. The solid-state fluorescence spectrum of compound **1** shows no emission bands under an excitation band of 365 nm. The energy of excited U(VI) ions is transferred to the organic triazololate ligand and quenched.⁵⁴

The U valence state of compound **1** was evaluated by X-ray photoelectron spectroscopy (XPS). The spectrum was collected in the 370–410 eV energy range after 10–20 s etching with an Ar^+ ion beam (Figure S5, Supporting Information). The spectrum was fit for U(VI) where the binding energies of U 4f_{7/2} and U 4f_{5/2} are at 382.215 and 393.096 eV, respectively. The fit parameters are comparable to corresponding values obtained in the spectra of other U(VI) compounds (Figure S5, Supporting Information),^{55,56} consistent with U(VI).

Thermal Stability. Thermogravimetric analysis (TG) of **1**, conducted over the temperature range 25–900 °C, is shown in Figure 3. The TG curve of **1** contains one significant weight

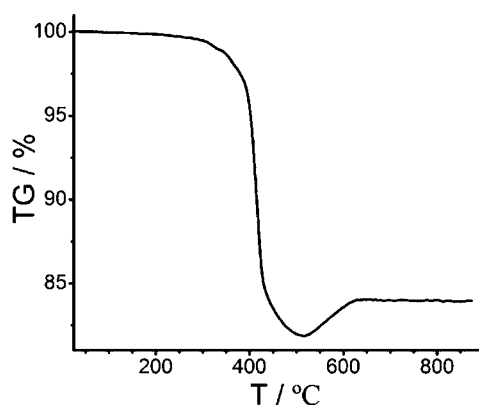


Figure 3. TG analysis of compound **1**.

loss, followed by a weight increase. The compound loses the organic ligand beginning at about 300 °C as well as some oxygen with a maximum weight loss at ~515 °C of 18.2%. Powder X-ray diffractometry for a sample cooled from 515 °C indicates the material is either $\text{UO}_{2.12}$ ⁵⁷ or a mixture of various UO_{2+x} phases (Figure S4, Supporting Information), consistent with reduction of the uranium from U(VI) to U(IV), presumably during oxidation of the organic component of the compound. With increasing temperature, the $\text{UO}_{2.12}$ or mixture of phases oxidizes in air with a weight gain of 2.1% by 620 °C. Subsequently, the weight remains constant between 620 and 900 °C, with a residue of 83.9% relative to the starting material. A room-temperature X-ray powder diffraction pattern of the residual cooled from 900 °C indicates it is $\alpha\text{-U}_3\text{O}_8$ (Figure S4, Supporting Information). Relative to **1**, the theoretical weight loss to $\text{UO}_{2.12}$ and $\alpha\text{-U}_3\text{O}_8$ is 19.6% and 17.0%, respectively, in reasonable agreement with the experimental data (18.2% and 16.1%, respectively).

Absorption Spectra of Compounds Adopting CCIs and Tetraoxido Cores. Typically, (UO_2)²⁺ in solution produces a vibrational-coupled electronic transition around 420 nm.⁵⁸ U(VI) has a 5f⁰ electron configuration; thus, the 420 nm signal is attributed to a singlet–triplet transition between the HOMO and the LUMO of (UO_2)²⁺ molecular orbitals that are derived by hybridization of U(VI) 5f and O²⁻ 2p orbitals.^{59–61} The intensity of this transition is of the same magnitude as f–f transitions. Both the intensity and the peak position of this transition vary with the chemical and

coordination environments about the U(VI) cation. The UV-vis spectrum is therefore useful for characterizing the speciation of U(VI) in solutions.⁵⁸ However, in solids, addition of crystal field splitting terms and crystal stacking preference effects make assignment of electronic transitions more challenging.

Figure 4 gives spectra collected for four U(VI) compounds that have distinct coordination environments about the U(VI)

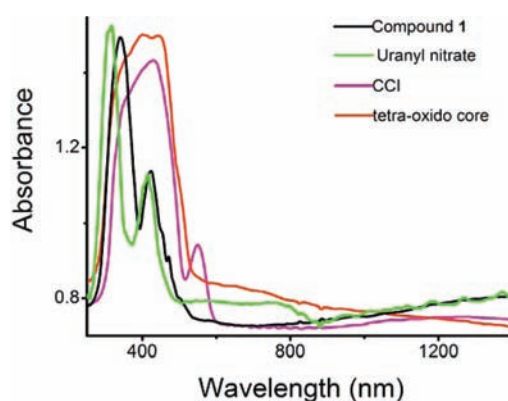


Figure 4. UV-vis absorption of compound 1, uranyl nitrate, compounds involving CCl,¹¹ and tetraoxido core.³⁶

sites. The spectrum for $\text{UO}_2(\text{NO}_3)_2 \cdot 6\text{H}_2\text{O}$, which contains a single U(VI) site that is a typical $(\text{UO}_2)^{2+}$ uranyl ion, exhibits a transition at ~ 420 nm (Figure 4) with a more intense peak also present at ~ 310 nm. The lower wavelength peak is also observed for U(VI) in solution but with more intensity. The structure of $\text{Ba}[(\text{UO}_6)_2(\text{UO}_2)_9(\text{GeO}_4)_2]$ ¹¹ contains three distinct U(VI) cations, two of which are present as typical $(\text{UO}_2)^{2+}$ uranyl ions and the third is in a distorted octahedral environment with bond lengths ranging from 2.041(7) to 2.109(7) Å. One of the uranyl ions in the structure donates a CCl. In the corresponding absorption spectrum there are two major peaks that are red shifted to higher wavelength regions (relative to $\text{UO}_2(\text{NO}_3)_2 \cdot 6\text{H}_2\text{O}$) at ~ 550 and ~ 430 nm, respectively (Figure 4). The peak at ~ 430 nm is broad and may correspond to multiple transitions. The compound $\text{Cd}_2(\text{H}_2\text{O})_2[\text{U}(\text{OH})(\text{CH}_3\text{COO})(\text{UO}_2)_5(\text{OH})_2\text{O}_8] \cdot 0.5\text{H}_2\text{O}$ ³⁶ contains U(VI) cations with six different coordination environments. Five of these correspond to typical $(\text{UO}_2)^{2+}$ uranyl ions in either square or pentagonal bipyramids, and the sixth is present as a U(VI) tetraoxido core. Its absorption spectrum contains one broad peak at ~ 420 nm that may correspond to several absorptions (Figure 4). This peak is similar to that for $\text{Ba}[(\text{UO}_6)_2(\text{UO}_2)_9(\text{GeO}_4)_2]$ except that it contains no peak at ~ 550 nm. The absorption spectrum of compound 1 is rather similar to that of $\text{UO}_2(\text{NO}_3)_2 \cdot 6\text{H}_2\text{O}$ but with a red shift, with

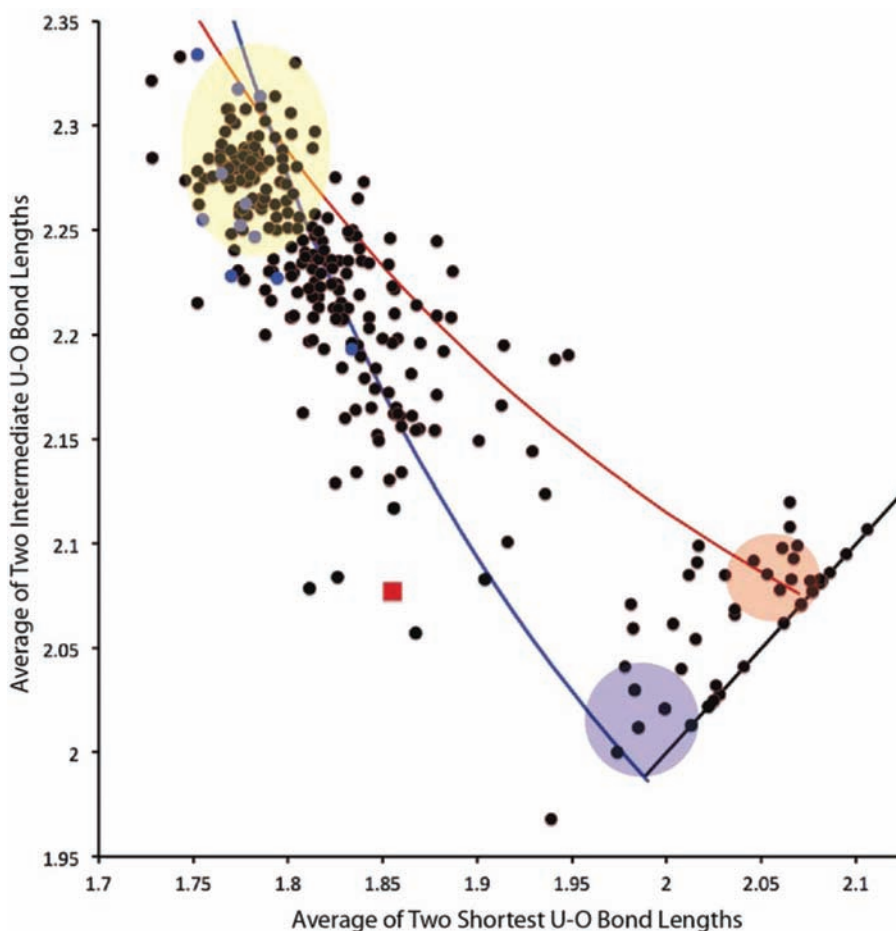


Figure 5. Bond length data for U(VI) cations coordinated by six O atoms extracted from the Inorganic Crystal Structure Database (black circles) and for U(VI) cations coordinated by four O atoms and two N atoms extracted from the Cambridge Structure Database (blue circles) (in Angstroms). Yellow, blue, and red fields correspond to typical uranyl square bipyramids, $(\text{UO}_4)^{2-}$ tetraoxido cores, and octahedra, respectively. Red and blue lines designate ideal pathways for the $2 + 4 \leftrightarrow 6$ and $2 + 4 \leftrightarrow 4 + 2$ pathways. U(2) site in compound 1 is represented by the red square.

peaks at ~ 340 and ~ 423 nm, although the red shift is not as great as that seen for $\text{Ba}[(\text{UO}_6)_2(\text{UO}_2)_9(\text{GeO}_4)_2]$. The spectrum for compound **1** also contains three shoulders at 455, 474, and 509 nm.

The absorption spectra for the four compounds shown in Figure 4 demonstrate the sensitivity of the transitions to the environment about the U(VI) cation. The presence of multiple U(VI) sites in all but $\text{UO}_2(\text{NO}_3)_2 \cdot 6\text{H}_2\text{O}$ leads to complex spectra with broader peaks in some cases. The peak at ~ 550 nm in the spectrum of $\text{Ba}[(\text{UO}_6)_2(\text{UO}_2)_9(\text{GeO}_4)_2]$ is at a longer wavelength than that observed for the other three compounds, and it may be related to the presence of either CCl₄ or the octahedral coordination of U(VI).

4. DISCUSSION

The $(\text{UO}_2)^{2+}$ uranyl ion dominates the crystal chemistry of U(VI) in oxygen-bearing compounds. Where the U(VI) cation is coordinated by a total of seven or eight O atoms, the uranyl ion is extremely common. In contrast, where there are six O atoms coordinating U(VI), considerable bond length variability is observed.⁴⁵

We retrieved bond length data for U(VI) coordinated by exactly six O atoms from the Inorganic Crystal Structure Database. The bond-valence sums were calculated for each site using coordination-specific parameters derived from well-refined structures.⁴⁵ Data for six compounds were discarded because the calculated bond-valence sums fell outside the range from 5.4 to 6.6 *vu*. Data for the remaining polyhedra are plotted in Figure 5 as black circles, which compares the average of the two shortest U(VI)–O bond lengths with the average of its two intermediate U(VI)–O bond lengths for each polyhedron. We also retrieved bond length data for U(VI) polyhedra containing exactly four O atoms and two N atoms from the Cambridge Structure Database and include these in Figure 5 where they are represented by blue circles.

The average U(VI)–O uranyl and equatorial bond lengths for six-coordinated polyhedra are 1.79(3) and 2.28(5) Å, corresponding to the population shaded in yellow in Figure 5.⁴⁵ The black line in Figure 5 denotes geometries in which the two averages are identical. The population that corresponds to mildly distorted or holosymmetric octahedra is shaded in red. The geometries of U(VI) tetraoxido cores reported in the literature fall in the blue shaded field.

We are interested in the geometries of six-coordinated U(VI) that are transitional between the colored fields in Figure 5, which correspond to the recognized coordination polyhedra. We define three coordination-geometry structural pathways, each shown by a line in Figure 5. That between the uranyl square bipyramid and the octahedron is designated $2 + 4 \leftrightarrow 6$ and involves an extension of the uranyl ion U(VI)–O bonds together with compression of all four of the U–O(eq) bonds. The pathway between the uranyl square bipyramid and the tetraoxido core is designated $2 + 4 \leftrightarrow 4 + 2$, as the U(VI) of the tetraoxido core is normally coordinated by two ligands in addition to those in the core. The third pathway is from a tetraoxido core to an octahedron, is designated $4 + 2 \leftrightarrow 6$, and shown by the black line in Figure 5. On the basis of the coordination-specific bond-valence parameters for six-coordinated U(VI),⁴⁵ the ideal pathways for $2 + 4 \leftrightarrow 6$ and $2 + 4 \leftrightarrow 4 + 2$ were calculated and are shown by red and blue lines, respectively.

The data in Figure 5 demonstrate that many of the six-coordinated U(VI) polyhedral geometries are transitional

between the “end-member” uranyl, tetraoxido, and octahedral geometries and that they are generally consistent with the proposed structural pathways defined here. The $2 + 4 \leftrightarrow 4 + 2$ structural pathway appears to be the most favored, although many of the distorted geometries are consistent with more than one structural pathway. The geometry of the U(2) site in compound **1** is shown by the red square in Figure 5. Two of the ligands are N with long U(VI)–N bonds, which results in shorter U(VI)–O bonds than for U(VI) polyhedra containing only O atoms. The data in Figure 5 support designation of the U(2) coordination geometry as a distorted tetraoxido core of the $2 + 4 \leftrightarrow 4 + 2$ structural pathway, intermediate between a uranyl square bipyramid and a tetraoxido core.

In summary, we synthesized and characterized an unusual U(VI) compound that contains two U(VI) coordination environments, one of which is transitional between a tetraoxido core and a uranyl square bipyramid. It contains electroneutral sheets of uranyl pentagonal bipyramids and the distorted U(VI) tetraoxido core, the latter of which is also coordinated by N atoms of the trz molecules. We emphasized the importance of coordination geometry transition pathways in the case of six-coordinated U(VI) polyhedra and demonstrated that many of the reported polyhedral geometries are not consistent with the “end-member” designations.

■ ASSOCIATED CONTENT

Supporting Information

Crystallographic data (CIF), powder X-ray diffraction pattern, and infrared, Raman, and X-ray photoelectron spectra of compound **1**. This material is available free of charge via the Internet at <http://pubs.acs.org>.

■ AUTHOR INFORMATION

Corresponding Author

*E-mail: pburns@nd.edu.

Notes

The authors declare no competing financial interest.

■ ACKNOWLEDGMENTS

This research was supported by the Chemical Sciences, Geosciences and Biosciences Division, Office of Basic Energy Sciences, Office of Science, U.S. Department of Energy, Grant No. DE-FG02-07ER15880.

■ REFERENCES

- (1) Burns, P. C.; Ewing, R. C.; Hawthorne, F. C. *Can. Mineral.* **1997**, *35*, 1551–1570.
- (2) Burns, P. C. *Can. Mineral.* **2005**, *43*, 1839–1894.
- (3) Burns, P. C.; Ikeda, Y.; Czerwinski, K. *MRS Bull.* **2010**, *35*, 868–876.
- (4) Forbes, T. Z.; Wallace, C.; Burns, P. C. *Can. Mineral.* **2008**, *46*, 1623–1645.
- (5) Burns, P. C. *Mineral. Mag.* **2011**, *75*, 1–25.
- (6) Arnold, P. L.; Patel, D.; Wilson, C.; Love, J. B. *Nature* **2008**, *451*, 315–317.
- (7) Boncella, J. M. *Nature* **2008**, *451*, 250–252.
- (8) Fox, A. R.; Bart, S. C.; Meyer, K.; Cummins, C. C. *Nature* **2008**, *455*, 341–349.
- (9) Evans, W. J.; Kozimor, S. A.; Ziller, J. W. *Science* **2005**, *309*, 1835–1838.
- (10) Hayton, T. W.; Boncella, J. M.; Scott, B. L.; Palmer, P. D.; Batista, E. R.; Hay, P. J. *Science* **2005**, *310*, 1941–1943.
- (11) Morrison, J. M.; Moore-Shay, L. J.; Burns, P. C. *Inorg. Chem.* **2011**, *50*, 2272–2277.

- (12) Severance, R. C.; Smith, M. D.; Loye, H.-C. z. *Inorg. Chem.* **2011**, *50*, 7931–7933.
- (13) Mihalcea, I.; Henry, N.; Clavier, N.; Dacheux, N.; Loiseau, T. *Inorg. Chem.* **2011**, *50*, 6243–6249.
- (14) Lhoste, J.; Henry, N.; Roussel, P.; Loiseau, T.; Abraham, F. *Dalton Trans* **2011**, *40*, 2422–2424.
- (15) Alekseev, E. V.; Krivovichev, S. V.; Depmeier, W. *J. Solid State Chem.* **2009**, *182*, 2977–2984.
- (16) Alekseev, E. V.; Krivovichev, S. V.; Depmeier, W.; Siidra, O. I.; Knorr, K.; Suleimanov, E. V.; Chuprunov, E. V. *Angew. Chem., Int. Ed.* **2006**, *45*, 7233–7235.
- (17) Alekseev, E. V.; Krivovichev, S. V.; Malcherek, T.; Depmeier, W. *Inorg. Chem.* **2007**, *46*, 8442–8444.
- (18) Sullens, T. A.; Jensen, R. A.; Shvareva, T. Y.; Albrecht-Schmitt, T. E. *J. Am. Chem. Soc.* **2004**, *126*, 2676–2677.
- (19) Kubatko, K.-A.; Burns, P. C. *Inorg. Chem.* **2006**, *45*, 10277–10281.
- (20) Sullivan, J. C.; Hindman, J. C.; Zielen, A. J. *J. Am. Chem. Soc.* **1961**, *83*, 3373–3378.
- (21) Stoyer, N. J.; Hoffman, D. C.; Silva, R. J. *Radiochim. Acta.* **2000**, *88*, 279–282.
- (22) Ekstrom, A. *Inorg. Chem.* **1974**, *13*, 2237–2241.
- (23) Guillaume, B.; Hobart, D. E.; Bourges, J. Y. *J. Inorg. Nucl. Chem.* **1981**, *43*, 3295–3299.
- (24) Mougél, V.; Horeglad, P.; Nocton, G.; Pécaut, J.; Mazzanti, M. *Angew. Chem., Int. Ed.* **2009**, *48*, 8477–8480.
- (25) Arnold, P. L.; Love, J. B.; Patel, D. *Coord. Chem. Rev.* **2009**, *253*, 1973–1978.
- (26) Nocton, G. g.; Horeglad, P.; Pécaut, J.; Mazzanti, M. *J. Am. Chem. Soc.* **2008**, *130*, 16633–16645.
- (27) Graves, C. R.; Kiplinger, J. L. *Chem. Commun.* **2009**, 3831–3853.
- (28) Fortier, S.; Hayton, T. W. *Coord. Chem. Rev.* **2010**, *254*, 197–214.
- (29) Nakamoto, T.; Nakada, M.; Nakamura, A.; Haga, Y.; Ōnuki, Y. *Solid State Commun.* **1998**, *109*, 77–81.
- (30) Wang, S.; Alekseev, E. V.; Depmeier, W.; Albrecht-Schmitt, T. E. *Inorg. Chem.* **2011**, *50*, 4692–4694.
- (31) Krivovichev, S.; Burns, P. C.; Tananaev, I. G. *Structural Chemistry of Inorganic Actinide Compounds*; Elsevier: Dordrecht, The Netherlands, 2007.
- (32) Forbes, T. Z.; Burns, P. C.; Skanthakumar, S.; Soderholm, L. *J. Am. Chem. Soc.* **2007**, *129*, 2760–2761.
- (33) Williams, C. W.; Blaudeau, J.-P.; Sullivan, J. C.; Antonio, M. R.; Bursten, B.; Soderholm, L. *J. Am. Chem. Soc.* **2001**, *123*, 4346–4347.
- (34) Bolvin, H.; Wahlgren, U.; Moll, H.; Reich, T.; Geipel, G.; Fanghänel, T.; Grenthe, I. *J. Phys. Chem. A* **2001**, *105*, 11441–11445.
- (35) Unruh, D. K.; Baranay, M.; Baranay, M.; Burns, P. C. *Inorg. Chem.* **2010**, *49*, 6793–6795.
- (36) Wu, S.; Ling, J.; Wang, S.; Skanthakumar, S.; Soderholm, L.; Albrecht-Schmitt, T. E.; Alekseev, E. V.; Krivovichev, S. V.; Depmeier, W. *Eur. J. Inorg. Chem.* **2009**, 4039–4042.
- (37) Brugger, J.; Krivovichev, S. V.; Berlepsch, P.; Meisser, N.; Ansermet, S.; Armbruster, T. *Am. Mineral.* **2004**, *89*, 339–347.
- (38) Li, Y.; Cahill, C. L.; Burns, P. C. *Chem. Mater.* **2001**, *13*, 4026–4031.
- (39) Macrae, C. F.; Bruno, I. J.; Chisholm, J. A.; Edgington, P. R.; McCabe, P.; Pidcock, E.; Rodriguez-Monge, L.; Taylor, R.; van de Streek, J.; Wood, P. A. *J. Appl. Crystallogr.* **2008**, *41*, 466–470.
- (40) Liu, J.-C.; Guo, G.-C.; Huang, J.-S.; You, X.-Z. *Inorg. Chem.* **2003**, *42*, 235–243.
- (41) Ouellette, W.; Prosvirin, A. V.; Chieffo, V.; Dunbar, K. R.; Hudson, B.; Zubieta, J. *Inorg. Chem.* **2006**, *45*, 9346–9366.
- (42) Li, N.; Chen, S.; Gao, S. *J. Coord. Chem.* **2007**, *60*, 117–123.
- (43) Weng, Z.-H.; Chen, Z.-L.; Liang, F.-P. *Acta Crystallogr.* **2008**, *C64*, M64–M66.
- (44) Ouellette, W.; Galán-Mascarós, J. R.; Dunbar, K. R.; Zubieta, J. *Inorg. Chem.* **2006**, *45*, 1909–1911.
- (45) Brese, N. E.; O’Keeffe, M. *Acta Crystallogr.* **1991**, *B47*, 192–197.
- (46) Burns, P. C.; Miller, M. L.; Ewing, R. C. *Can. Mineral.* **1996**, *34*, 845–880.
- (47) Siegel, S.; Viste, A.; Hoekstra, H. R.; Tani, B. *Acta Crystallogr.* **1972**, *B28*, 117–121.
- (48) Saine, M. C. *J. Less-Common Met.* **1989**, *154*, 361–365.
- (49) Borello, E.; Zecchina, A. *Spectrochim. Acta* **1963**, *19*, 1703–1715.
- (50) Bougeard, D.; Calvé, N. L.; Roch, B. S.; Novak, A. *J. Chem. Phys.* **1976**, *64*, 5152.
- (51) Bullock, J. I. *J. Inorg. Nucl. Chem.* **1967**, *29*, 2257–2264.
- (52) Frost, R. L.; Dickfos, M. J.; Čejka, J. *J. Raman Spectrosc.* **2008**, *39*, 1158.
- (53) Bartlett, J. R.; Cooney, R. P. *J. Mol. Struct.* **1989**, *193*, 295–300.
- (54) Meinrath, G. *J. Radioanal. Nucl. Chem.* **1997**, *224*, 119–126.
- (55) Lee, C.-S.; Lin, C.-H.; Wang, S.-L.; Lii, K.-H. *Angew. Chem., Int. Ed.* **2010**, *49*, 4254–4256.
- (56) Liu, J.-H.; Berghe, S. V. d.; Konstantinović, M. J. *J. Solid State Chem.* **2009**, *182*, 1105–1108.
- (57) Willis, B. T. M. *Acta Crystallogr.* **1978**, *A34*, 88–90.
- (58) Meinrath, G. *J. Radioanal. Nucl. Chem.* **1997**, *224*, 119–126.
- (59) Jeżowska-Trzebiatowska, B.; Bartecki, A. *Spectrochim. Acta* **1962**, *18*, 799–807.
- (60) Brint, P.; McCaffery, A. *J. Mol. Phys.* **1973**, *25*, 311–322.
- (61) McGlynn, S. P.; Smith, J. K. *J. Mol. Spectrosc.* **1961**, *6*, 164–187.